Uncovering human METTL12 as a mitochondrial methyltransferase that modulates citrate synthase activity through metabolite-sensitive lysine methylation

Received for publication, July 26, 2017, and in revised form, August 28, 2017 Published, Papers in Press, September 8, 2017, DOI 10.1074/jbc.M117.808451

Jędrzej Małecki[‡], Magnus E. Jakobsson[‡1], Angela Y. Y. Ho[‡], Anders Moen[‡], Arild C. Rustan[§], and Pål Ø. Falnes[‡2]

From the [‡]Department of Biosciences and [§]School of Pharmacy, Faculty of Mathematics and Natural Sciences, University of Oslo, 0316 Oslo, Norway

Edited by John M. Denu

Lysine methylation is an important and much-studied post-translational modification of nuclear and cytosolic proteins but is present also in mitochondria. However, the responsible mitochondrial lysine-specific methyltransferases (KMTs) remain largely elusive. Here, we investigated METTL12, a mitochondrial human *S*-adenosylmethionine (AdoMet)-dependent methyltransferase and found it to methylate a single protein in mitochondrial extracts, identified as citrate synthase (CS). Using several *in vitro* and *in vivo* approaches, we demonstrated that METTL12 methylates CS on Lys-395, which is localized in the CS active site. Interestingly, the METTL12-mediated methylation inhibited CS activity and was blocked by the CS substrate oxaloacetate. Moreover, METTL12 was strongly inhibited by the reaction product *S*-adenosylhomocysteine (AdoHcy). In summary, we have uncovered a novel human mitochondrial KMT that introduces a methyl modification into a metabolic enzyme and whose activity can be modulated by metabolic cues. Based on the established naming nomenclature for similar enzymes, we suggest that METTL12 be renamed CS-KMT (gene name *CSKMT*).

Many biomolecules ranging from small metabolites to nucleic acids and proteins are subject to methylation by methyltransferases (MTases)[3] that use *S*-adenosylmethionine (AdoMet) as the methyl donor (1). The products of the AdoMet-dependent MTase reaction are the methylated substrate and *S*-adenosylhomocysteine (AdoHcy), which for some MTases competitively inhibits AdoMet binding (2, 3). In proteins, several amino acid residues can be targeted for methylation, including glutamine, histidine, arginine, and lysine (4–7). Lysine (K)-specific MTases (KMTs) catalyze the transfer of up to three methyl groups to the ϵ-amino group of lysine, resulting in mono-, di-, or trimethyllysine (8–10). As more methyl groups are being attached, the overall charge of the lysine residue remains unaffected, but the bulkiness increases, and the hydrogen bonding capability is reduced.

Lysine methylation has been shown to modulate many aspects of protein function, such as protein-protein interactions, enzymatic activity, and protein stability. The functional importance of lysine methylation has been most intensively studied for histone methylation by KMTs that contain a defining SET (Su(var)3–9, Enhancer-of-zeste, Trithorax) domain (9). Methylation of specific lysines in histone tails has been established as an important determinant of chromatin state and gene expression, and together with other post-translational modifications constitute the so-called "histone code" (11). However, lysine methylation on non-histone proteins is also common, and in fact numerous non-histone proteins have been identified as substrates for many of the SET enzymes (6).

In addition, several members of a different MTase class, the so-called seven β-strand (7BS) MTases, have recently been established as KMTs that target various non-histone proteins (8). These include members of the so-called methyltransferase family 16 (MTF16), which all share a characteristic and conserved D*XX*Y motif (consensus: (D/E)*XX*(Y/F)), located directly downstream of the fourth β strand of the 7BS fold (12). The corresponding region, referred to as motif "Post II," has been implicated in catalysis and substrate specificity (8). Until now, 7 of 10 human MTF16 members were established as KMTs, suggesting that the remaining three members are also KMTs (12–19). Moreover, two human (non-MTF16) 7BS MTases, denoted eEF1A-KMT2 (gene name *EEF1AKMT2*; alias *METTL10*) and eEF1A-KMT4 (gene name *EEF1AKMT4*; alias *ECE2*) were demonstrated to methylate eukaryotic elongation factor 1α (eEF1A) on Lys-318 and Lys-36, respectively (20, 21). Together with the two yet uncharacterized 7BS MTases METTL12 and METTL13, these two enzymes were recently reported to constitute the human members of a novel putative KMT family, defined by a common motif Post II of consensus (D/E)KGT*X*D (20).

This work was supported by grants from the Research Council of Norway (FRIMEDBIO-240009] and the Norwegian Cancer Society (107744-PR-2007–0132). The authors declare that they have no conflicts of interest with the contents of this article.

This article contains supplemental Figs. S1–S3.

[1] Present address: Proteomics Program, Faculty of Health and Medical Sciences, Novo Nordisk Foundation Center for Protein Research, University of Copenhagen, Blegdamsvej 3B, 2200 Copenhagen, Denmark.

[2] To whom correspondence should be addressed. Tel.: 47-91151935; E-mail: pal.falnes@ibv.uio.no.

[3] The abbreviations used are: MTase, methyltransferase; 7BS, seven β-strand; AdoHcy, *S*-adenosylhomocysteine; AdoHcyase, AdoHcy hydrolase; AdoMet, *S*-adenosylmethionine; CS, citrate synthase; TNB, 5-thio-2-nitrobenzoic acid; DTNB, 5,5-dithiobis-(2-nitrobenzoic acid); EGFP, enhanced green fluorescent protein; KMT, lysine-specific methyltransferase; MTF16, methyltransferase family 16; MTS, mitochondrial targeting sequence; SET, Su(var)3–9, Enhancer-of-zeste, Trithorax; TUFM, mitochondrial elongation factor Tu; OAA, oxaloacetate; WT, wild type; eEF1A, eukaryotic elongation factor 1α; ETFβ, β-subunit of electron transfer flavoprotein.

Thus far, only a single human mitochondrial KMT has been characterized, namely ETFβ-KMT (gene name *ETFBKMT*; alias *METTL20*), which is a member of MTF16 and targets Lys-200 and Lys-203 in the β-subunit of electron transfer flavoprotein (ETFβ) (17, 19). However, many mitochondrial proteins have been shown to contain methylated lysine residues, and several uncharacterized MTases have a predicted mitochondrial localization, suggesting the existence of additional mitochondrial KMTs (22, 23). One interesting candidate is METTL12, which shows sequence similarity to established KMTs and has a predicted mitochondrial localization (20, 23).

Citrate synthase (CS) resides in the mitochondrial matrix where it catalyzes the condensation of oxaloacetate (OAA) with acetyl-CoA to form citrate and CoA, *i.e.* the first committed and irreversible step of the Krebs cycle. Numerous studies have investigated the regulation of CS activity (24–26). It is generally accepted that the overall rate of the CS-catalyzed reaction is mainly determined by the availability of the substrates acetyl-CoA and OAA, which are usually present in mitochondria at concentrations much lower than those required to saturate CS. In addition, CS was reported to be inhibited by citrate and succinyl-CoA (27, 28). So far, regulation of CS activity by post-translational modification has not been reported. However, mammalian CS has been reported to be subject to lysine methylation; CS from both human and pig were reported to be trimethylated at Lys-395 (22, 29) (amino acid numbering according to UniProt), which is localized in the CS active site (30).

In the present study we have taken an activity-based approach to establish the function of METTL12. We detected a single substrate for recombinant METTL12 in *METTL12* knock-out (KO) cell extracts, and we found this substrate to be CS. Through extensive *in vitro* and *in vivo* studies we demonstrate that METTL12 is responsible for methylation of Lys-395 in CS. We also found that CS activity was diminished by methylation and that METTL12-dependent methylation was inhibited by OAA and AdoHcy.

Experimental procedures

Cloning and mutagenesis

Cloning of human open reading frames and mutagenesis were performed as described previously (17). All constructs were sequence-verified.

Bioinformatics analysis

NCBI Basic Local Alignment Search Tool (BLAST) was used to identify protein sequences homologous to human METTL12 (31). Multiple sequence alignments were generated using algorithms embedded in the Jalview (v2.8) interface (32).

Cell cultivation and generation of stable cell lines

Human cell lines were grown at standard conditions, typically in DMEM GlutaMAX medium supplemented with 10% (v/v) fetal bovine serum (FBS), 100 units/ml of penicillin, and 0.1 mg/ml streptomycin (P/S). Human HAP1 cells were grown in Iscove's modified Dulbecco's GlutaMAX medium (IMDM) supplemented with 10% FBS and P/S. The generation of *METTL12* KO HAP1 cells was initiated as a custom (non-exclusive) project with Horizon Genomics (Vienna, Austria), and these cells are now commercially available (Horizon Discovery HZGHC000536c011). Genomic ablation of the *METTL12* gene was performed using the CRISPR-Cas9 technology, with guide RNA designed to target the *METTL12* gene upstream of motif "Post I" (Fig. 2*A*). Individual clones were selected by limiting dilution, and frame-shifting events within the *METTL12* gene were determined by sequencing of genomic DNA. Complementation of *METTL12* KO cells was performed by transfecting cells with a p3×FLAG-CMV-14-derived plasmid that encoded either wild-type or D107A-mutated C-terminally 3×FLAG-tagged METTL12 using the FuGENE6 Transfection Reagent (Roche Applied Science). Transfected cells were selected with 1 mg/ml Geneticin (Gibco) and expanded in medium containing Geneticin. Individual clones were screened by Western blot for the presence of 3×FLAG tag, citrate synthase (CS), and GAPDH (as loading control) using anti-FLAG (Sigma, F1804), anti-citrate synthase (Proteintech, 16131-1-AP), and anti-GAPDH (Abcam, ab9485) antibodies, respectively.

Transient transfection and fluorescence microscopy

HeLa cells were transiently transfected with pEGFP-N1-derived plasmids (Clontech), encoding human full-length METTL12 or only its N terminus (consisting of amino acids 1–30) fused to the N terminus of enhanced green fluorescent protein (EGFP). Cells were analyzed by confocal fluorescence microscopy 24 h after transfection. Living cells were stained with 50 nM MitoTracker Deep Red FM (Life Technologies) and 0.5 μg/ml Hoechst 33258 (Sigma) to visualize the mitochondria and the nuclei, respectively. Cells were imaged using an Olympus FluoView 1000 (Ix81) confocal fluorescence microscopy system with a PlanApo 60× NA 1.1 oil objective (Olympus). The different fluorophores were excited at 405 nm (Hoechst), 488 nm (EGFP), and 635 nm (MitoTracker), and Kalman averaging ($n = 3$) was used to record multichannel images. The fluorescent signals emitted from EGFP, MitoTracker, and Hoechst were acquired through green, red, and blue channels, respectively, and merged.

Expression and purification of recombinant His-tagged proteins

Human Δ28 METTL12, Δ27 citrate synthase, and Δ43 TUFM (mature forms lacking a mitochondrial targeting sequence (MTS), with the indicated N-terminal amino acids deleted) were cloned into the pET28a plasmid for expression as N-terminally 6×His-tagged proteins. Protein expression in the *Escherichia coli* strain BL21-CodonPlus(DE3)-RIPL (Agilent Technologies) was induced with 0.1 mM isopropyl 1-thio-β-D-galactopyranoside at 16 °C overnight. Bacteria were lysed in lysis buffer (50 mM Tris-HCl, pH 7.4, 100 mM NaCl, 5% glycerol, 1% Triton X-100) supplemented with 2 mM 2-mercaptoethonol, 30 mM imidazole, 1× Complete (EDTA-free) protease inhibitor mixture (Roche Applied Science), and 10 units/ml Benzonase nuclease (Sigma), and the His-tagged proteins were purified on nickel-nitrilotriacetic acid-agarose (Qiagen) according to the manufacturer's instructions. Eluted proteins

were buffer-exchanged to storage buffer (50 mM Tris-HCl, pH 7.4, 100 mM NaCl, and 10% glycerol) using centrifugal concentrators with a molecular mass cut-off of 10 kDa (Sartorius). Recombinant METTL12 was additionally purified by anion-exchange using the ÄKTA HPLC system and loaded on HiTrap Q HP column (GE Healthcare) equilibrated in equilibration buffer (50 mM Tris-HCl, pH 7.4, 100 mM NaCl). METTL12 was eluted from the column at ~0.3 M KCl using a linear gradient of KCl (between 0 and 1.0 M) in equilibration buffer and finally buffer-exchanged to storage buffer.

Proteins were >90% pure as assessed by SDS-PAGE and Coomassie Blue staining. Protein concentrations were measured using Pierce BCA protein assay kit (Thermo Fisher Scientific).

Preparation and fractionation of cell extracts

Crude mitochondria-enriched (mitochondrial) fraction was prepared using the Mitochondria Isolation Kit for Cultured Cells (Thermo Fisher Scientific) according to the manufacturer's instructions by following the reagent-based protocol.

Human cells or mitochondrial fractions were lysed for 5 min at 4 °C in lysis buffer supplemented with 1 mM dithiothreitol and protease inhibitor mixture (catalog no. P8340; Sigma), and the resulting lysates were cleared by centrifugation. Samples of frozen pig organs were fragmented mechanically, lysed in lysis buffer (supplemented as above), sonicated, and cleared by centrifugation.

Mitochondrial or whole-cell extracts were fractionated at 4 °C by ion-exchange chromatography using the Pierce Strong Cation Exchange (S) Spin Column (Thermo Fisher Scientific). First, NaCl concentration was reduced to 50 mM by diluting cell lysates with dilution buffer (50 mM Tris-HCl, pH 7.4, 5% glycerol), and then extracts were applied onto S-column equilibrated in dilution buffer. Material bound to the S-column was eluted in 100-μl aliquots by a step gradient of increasing NaCl concentrations prepared in dilution buffer, similarly as previously described (33).

In vitro methyltransferase assay using [^{3}H]AdoMet

To test the MTase activity of METTL12 on cellular material, 10-μl reactions were assembled on ice containing 1× storage buffer, 50 pmol of recombinant METTL12, 40–60 μg of protein from cell extracts, and 0.5 μCi of [^{3}H]AdoMet (Perkin-Elmer Life Sciences) ($[AdoMet]_{total}$ = 0.64 μM, specific activity = 78.2 Ci/mmol). Reaction mixtures were incubated at 30 °C for 1 h and analyzed by SDS-PAGE and fluorography, similarly as previously described (18). Typically, fluorography experiments were performed three times, with similar results, and data from a representative experiment are shown.

For scintillation counting and titration experiments, MTase reactions contained [^{3}H]AdoMet, which was diluted with non-radioactive AdoMet (New England BioLabs). In this case, reaction mixtures (10 μl) contained 1× storage buffer, 0.5 μCi of [^{3}H]AdoMet, 32 μM AdoMet, varying amounts of recombinant METTL12 (0–200 pmol), and a fixed amount of recombinant CS (20 pmol). Reactions were stopped by adding 1 ml of 10% trichloroacetic acid (TCA), and TCA-insoluble material was subjected to scintillation counting.

Preparation of samples for MS analysis

In vitro methylation of recombinant or cellular (in extract) proteins, for the purpose of mass spectrometry (MS) analysis, was performed as in the above section, except that [^{3}H]AdoMet was replaced with nonradioactive AdoMet (1 mM). When indicated, the methylation reaction contained additionally 1 unit/ml AdoHcy hydrolase (AdoHcyase) from rabbit erythrocytes (Sigma). CS present in extracts was up-concentrated by loading cleared lysates on the S-column and eluting bound material with elution buffer (50 mM Tris-HCl, pH 7.4, 150 mM NaCl, 5% glycerol) with added protease inhibitor mixture. Proteins were resolved by SDS-PAGE and stained with Coomassie, the portion of gel containing the protein of interest was excised and subjected to in-gel trypsin (Sigma) or chymotrypsin (Roche Applied Science) digestion, and the resulting proteolytic fragments were analyzed by liquid chromatography MS, similarly as previously described (18).

MS data were analyzed using an in-house-maintained human and pig protein sequence databases using SEQUEST™ and Proteome Discoverer™ (Thermo Fisher Scientific). The mass tolerances of a fragment ion and a parent ion were set as 0.5 Da and 10 ppm, respectively. Methionine oxidation, cysteine carbamidomethylation, and lysine and arginine methylation were selected as variable modifications. MS/MS spectra of peptides corresponding to methylated CS were manually searched by Qual Browser (v2.0.7).

Citrate synthase activity assay

The activity of CS was assayed by reaction of 5,5-dithiobis-(2-nitrobenzoic acid) (DTNB) with the free thiol group of CoA (generated as result of citrate formation from OAA and acetyl-CoA), which leads to formation of yellow 5-thio-2-nitrobenzoic acid (TNB) that is detected spectrophotometrically at 412 nm (34). To determine the effect of METTL12-mediated methylation on CS enzymatic activity, 0.5 μM CS was incubated for 1 h at 30 °C with 2 μM METTL12, either wild-type or D107A-mutated, in the absence or presence of 1 mM AdoMet or AdoHcy, all in 1× storage buffer. Next, the incubation mixture was diluted 250× in storage buffer supplemented with 100 μM DTNB and 300 μM acetyl-CoA. Samples were left to equilibrate at room temperature for 1 min, and then the reaction was started by adding 300 μM OAA through manual mixing. For titration experiments the reaction was started by adding varying amounts of OAA. The kinetics of TNB formation was monitored continuously at 412 nm for 1 min using a Shimadzu UV-1601 spectrophotometer, and the initial rate of reaction was calculated from the slope of the linear part of the kinetic curve and expressed as change in absorption at 412 nm/min (ΔA_{412}/min). When indicated, the results from individual experiments were normalized for the activity of CS in the appropriate control and averaged.

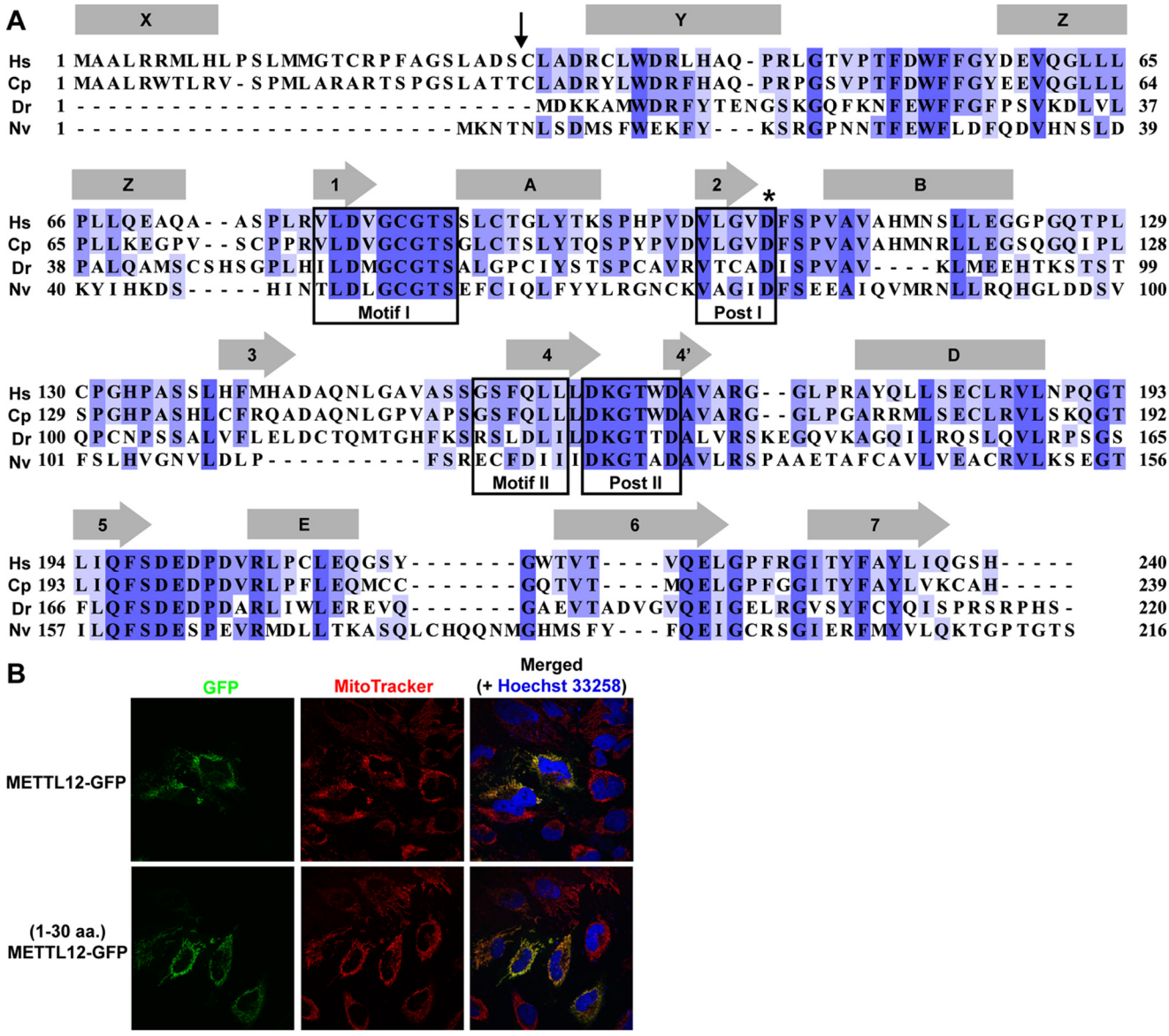

Figure 1. METTL12 is an evolutionary conserved mitochondrial 7BS protein. *A*, alignment of putative METTL12 orthologues from *Homo sapiens* (*Hs*; NP_001036694.1), *Cavia porcellus* (*Cp*; XP_003467900.2), *Danio rerio* (*Dr*; NP_001018613.1), and *Nematostella vectensis* (*Nv*; XP_001636263.1). Predicted α-helixes (*rectangles*) and β-strands (*arrows*) are indicated. Hallmark motifs found in 7BS MTases are *boxed*. The *vertical arrow* shows the predicted position of cleavage of the putative MTS in human METTL12. The position of conserved aspartate (Asp-107) crucial for AdoMet binding is indicated with an *asterisk*. *B*, *in vivo* confocal fluorescence microscopy images of HeLa cells after 24 h of transient transfection expressing either METTL12-GFP or (1–30)-METTL12-GFP in the presence of MitoTracker and Hoechst dyes. Data were acquired through *green* (GFP), *red* (MitoTracker), and *blue* (Hoechst) channels and merged. *aa*, amino acids.

Statistical analysis

The independent two-sample Student's *t* test was used to evaluate the probability (*p* value) that the means of two populations are not different.

Results

METTL12 is a mitochondrial 7BS MTase mainly found in vertebrates

We recently reported that the uncharacterized human 7BS MTase METTL12 is likely a KMT due to its sequence similarity with other established human KMTs (20). Also, METTL12 contains a putative MTS (23) and because only a single mitochondrial KMT has been characterized thus far, we found it of particular interest to investigate the function of METTL12.

Protein sequence searches revealed that putative METTL12 orthologues are mainly restricted to vertebrates, where they show a somewhat scattered evolutionary distribution, but they are also present in some invertebrate animals (Fig. 1*A*). Among mammals, METTL12 can be found in human, cow, and pig, but it is present only in a subset of rodents, *e.g.* it is found in guinea pig, but is absent in rat and mouse. An alignment of METTL12 orthologues revealed the presence of conserved hallmark motifs characteristic for 7BS MTases, such as Motif I, Post I, and Motif II (Fig. 1*A*) (35), as well as the specificity-associated motif Post II, which is very similar to that found in eEF1AKMT2, eEF1AKMT4, and METTL13 (20).

By using the MitoProt algorithm (36) we found that METTL12 is likely localized to mitochondria, as the initial ~28

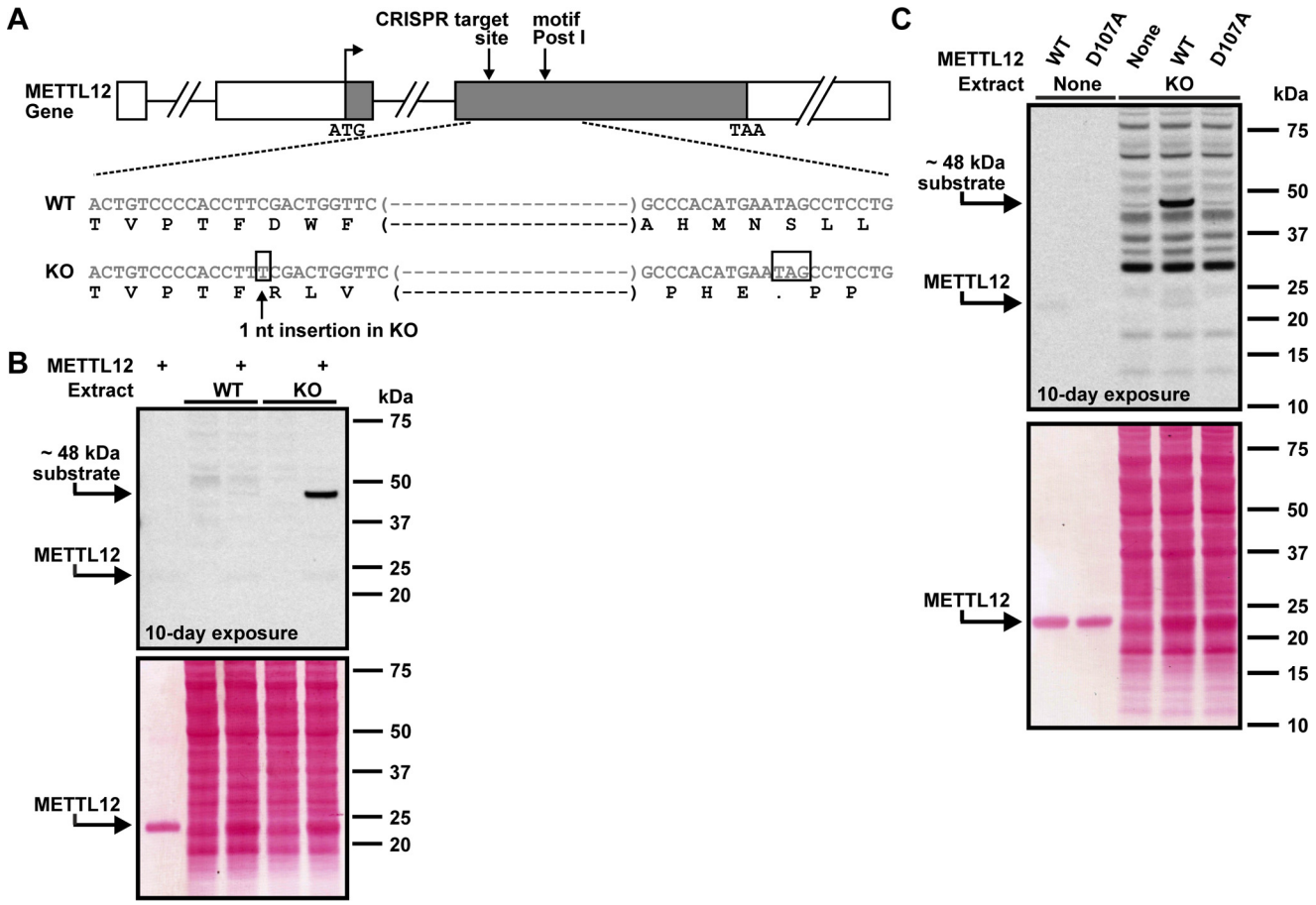

Figure 2. Human METTL12 is a protein-specific MTase. *A*, targeting of *METTL12* gene in human HAP1 WT cells by CRISPR/Cas9 generated *METTL12* KO cells containing a 1 base pair insertion in the *METTL12* gene, located upstream of motif Post I, resulting in generation of truncated METTL12 protein. The *dashed lines* interrupting the open reading frames correspond to 177 nucleotides, *i.e.* 59 amino acids. *B*, METTL12-dependent protein methylation in cell extracts. Mitochondrial extracts from HAP1 WT or *METTL12* KO cells were incubated with [^{3}H]AdoMet and recombinant human METTL12. Methylation reactions were separated by SDS-PAGE and transferred to a membrane. Methylation was visualized by fluorography (*top*) of the Ponceau S-stained membrane (*bottom*). *Arrows* indicate the positions of the ~48 kDa substrate and METTL12. *C*, D107A mutation abrogates enzymatic activity of METTL12. Mitochondrial extracts from *METTL12* KO cells were incubated with [^{3}H]AdoMet and recombinant human METTL12, either WT or D107A-mutated. Methylation was analyzed as in *B*. Note: in *panels B* and *C* different levels of background (non-METTL12-dependent) methylation are observed; this is likely due to differences in the purity of the mitochondrial extracts.

N-terminal amino acids of METTL12 were predicted to represent a MTS. Indeed, both the full-length METTL12 and the isolated putative MTS were, when expressed as N-terminal fusions with GFP, able to target GFP to mitochondria, thus confirming that METTL12 is a mitochondrial protein (Fig. 1*B*).

Generation of METTL12 KO cells and demonstration of protein MTase activity

To functionally characterize METTL12, the *METTL12* gene was disrupted in the haploid HAP1 cells using CRISPR/Cas9 technology. Abrogation of the *METTL12* gene function was assured by designing a guide RNA to target a sequence located upstream of motif Post I, which contains a catalytically important acidic residue (*i.e.* Asp-107 in METTL12) that is crucial for AdoMet binding in 7BS MTases (12, 15, 17, 20). Through DNA sequencing, a clone was identified that carried a 1-bp insertion at the target site, resulting in a shifted reading frame. This mutant gene encodes a predicted protein encompassing the 51 N-terminal amino acids of METTL12 followed by 66 residues resulting from out-of-frame translation. The mutant protein is thus severely truncated relative to the wild-type protein (240 amino acids) and highly likely inactive (Fig. 2*A*).

Previously, we showed that many recombinant human KMT enzymes can methylate their respective substrates in a cellular extract (14, 15, 17, 18). In several cases, such methylation was much more prominent in extracts from corresponding KMT KO cells, due to the substrate being exclusively in an unmethylated state. Consequently, we tested the ability of recombinant METTL12 to methylate proteins in a mitochondria-enriched extract from *METTL12* KO cells. For this purpose we used a truncated version of METTL12 that lacked the 28 N-terminal amino acids predicted to represent the mature, MTS-less version of the protein. The methylation reactions were performed in the presence of [^{3}H]AdoMet and then analyzed by SDS-PAGE and fluorography, enabling the visualization of methylated proteins as distinct bands. Interestingly, we detected radiolabeling of a protein with an apparent molecular mass of ~48 kDa upon incubation of METTL12 with the extract from KO cells. No such labeling was observed when the wild-type (WT) HAP1 cells were used (Fig. 2*B*), indicating that the 48 kDa band represents a true METTL12 substrate. A putatively enzymatically inactive mutant of METTL12 (D107A) was used as a negative control, and, reassuringly, we did not detect any label-

ing of the ~48 kDa substrate when this mutant enzyme was used, excluding the possibility that the observed labeling was mediated by an *E. coli*-derived contaminant (Fig. 2*C*). In addition we detected after longer exposures weak automethylation of METTL12 similar to what has been observed for many other KMTs (12, 17, 20, 33). In summary, these results show that METTL12 is a mitochondrial enzyme with protein MTase activity.

Identification of citrate synthase as a likely substrate of human METTL12

To reveal the identity of the ~48-kDa substrate, we incubated mitochondrial extracts from *METTL12* KO cells with [^{3}H]AdoMet and recombinant METTL12 and then subjected the reaction mixtures to fractionation on a cation-exchange (S) column (Fig. 3*A*). A parallel sample where wild-type recombinant METTL12 had been replaced by the enzymatically inactive mutant D107A was subjected to the same fractionation scheme, thus representing a negative control. We found that the ~48-kDa ^{3}H-labeled protein bound to the S-column was optimally eluted between 0.05 and 0.15 M NaCl (denoted as the 0.15 fraction) (Fig. 3*B*). To identify the METTL12 substrate, the *METTL12* KO extract was fractionated (in the absence of radioactivity), the 0.15 fraction was resolved by SDS-PAGE, and the ~48-kDa region was excised from the gel (Fig. 3*C*) followed by trypsin digestion and protein identification by MS. Among several mitochondrial proteins that were identified (Table 1), only one, namely citrate synthase, had been reported in the literature as being methylated on lysine. CS contains a trimethylated lysine residue in position 368 in the mature protein corresponding to Lys-395 in the CS precursor (29). The latter numbering is used in protein databases such as UniProt and PhosphoSitePlus (post-translational modifications) and will also be used here by us. The molecular weight of mature CS (49 kDa) matched that of the methylated substrate detected by fluorography, and when an anti-CS antibody was used to detect CS throughout fractionation, it was found that the elution profile of CS was indistinguishable from that of the ~48-kDa substrate (compare Fig. 3, *B* and *C*).

To further investigate the potential ability of METTL12 to methylate CS, we incubated the *METTL12* KO cell extract with recombinant METTL12, then subjected the extract to fractionation, and the methylation status of Lys-395 in CS from the 0.15 fraction was assessed by MS. Strikingly, we found that Lys-395 was exclusively unmethylated in the KO cells (Fig. 3, *D* and *E*), whereas treatment with recombinant METTL12 shifted Lys-395 to the trimethylated (Me3) and dimethylated (Me2) states (Fig. 3, *D* and *E*). This demonstrates that METTL12 can methylate Lys-395 in CS *in vitro* and suggests that the enzyme is responsible for CS methylation also *in vivo*.

METTL12 catalyzes methylation of Lys-395 in CS in vitro

To further investigate CS as a substrate for METTL12-mediated methylation *in vitro*, we expressed and purified mature (MTS-less) CS in *E. coli*, and the resulting recombinant protein was then tested as a substrate for METTL12-mediated methylation. Clearly, METTL12 methylated recombinant CS *in vitro*, but a rather high amount of enzyme relative to substrate (>2-fold excess) was required to obtain maximal methylation (Fig. 4*A*). Importantly, protein mass spectrometry demonstrated the presence of trimethylated Lys-395 in recombinant CS that had been treated with METTL12, whereas Lys-395 was found to be unmethylated in untreated CS (supplemental Fig. S1). We also replaced Lys-395 by arginine in recombinant CS, which completely abolished methylation, indicating that Lys-395 is the only methylation site (Fig. 4*B*). Moreover, we considered the possibility that also a neighboring lysine residue, Lys-393, may be subject to methylation. However, this appears not to be the case, as methylation was not affected by mutation at this position (Fig. 4*B*) and because we were unable to find evidence for such methylation in the MS data. Taken together, the above data demonstrate that METTL12 catalyzes methylation of CS at Lys-395 *in vitro*.

Processivity, turnover, and metabolite modulation of METTL12-mediated methylation

Many KMTs that introduce trimethylation on their target lysines have a distributive mode of action, *i.e.* they introduce a single methyl group per binding event, thus generating a mixture of methylation states at lower enzyme concentrations. In contrast, other trimethylating KMTs are processive, *i.e.* they introduce all three methyl groups during a single binding event and thus exclusively generate the trimethylated product. To investigate the mode of action of METTL12, we incubated recombinant CS with different amounts of METTL12 and assessed the methylation status of Lys-395 by MS using extracted ion chromatograms corresponding to the various methylation states of a Lys-395-encompassing peptide (Leu-389–Leu-408). Treatment of CS with a large excess of METTL12 predominantly yielded the trimethylated state, but when equimolar amounts of CS and METTL12 were used a mixture of the methylation states was observed, clearly demonstrating that METTL12 has a distributive mode of action (Fig. 5*A*, *upper panel*).

We noted that METTL12 enzyme was relatively inefficient and appeared incapable of performing catalytic turnover; at limiting enzyme concentrations, one MTase molecule mediated, on average, the incorporation of (approximately) a single methyl group (Fig. 5*B*). Many AdoMet-dependent MTases are inhibited by the byproduct AdoHcy (the demethylated counterpart of AdoMet) (3), and we, therefore, considered the possibility that inhibition of METTL12 by AdoHcy may prevent catalytic turnover. To test this we added AdoHcyase, which catalyzes the hydrolysis of AdoHcy, to the reaction mixture for METTL12-mediated methylation of CS. Clearly, the addition of AdoHcyase dramatically increased the efficiency of methylation and improved the catalytic turnover (Fig. 5, *A* and *B*). These results indicate that AdoHcy generated in the methylation reaction has a strong inhibitory effect on METTL12.

To further investigate the influence of AdoHcy on METTL12 activity, we performed *in vitro* methylation reactions where the concentrations of CS, METTL12, and AdoMet were held constant (at 2 μM, 2 μM, and 32.6 μM respectively) whereas the concentration of AdoHcy was varied (0–300 μM). The results showed that METTL12-mediated methylation of CS was strongly inhibited by the addition of AdoHcy (Fig. 5*C*); visible inhibition was observed already at 1 μM AdoHcy, and methyl-

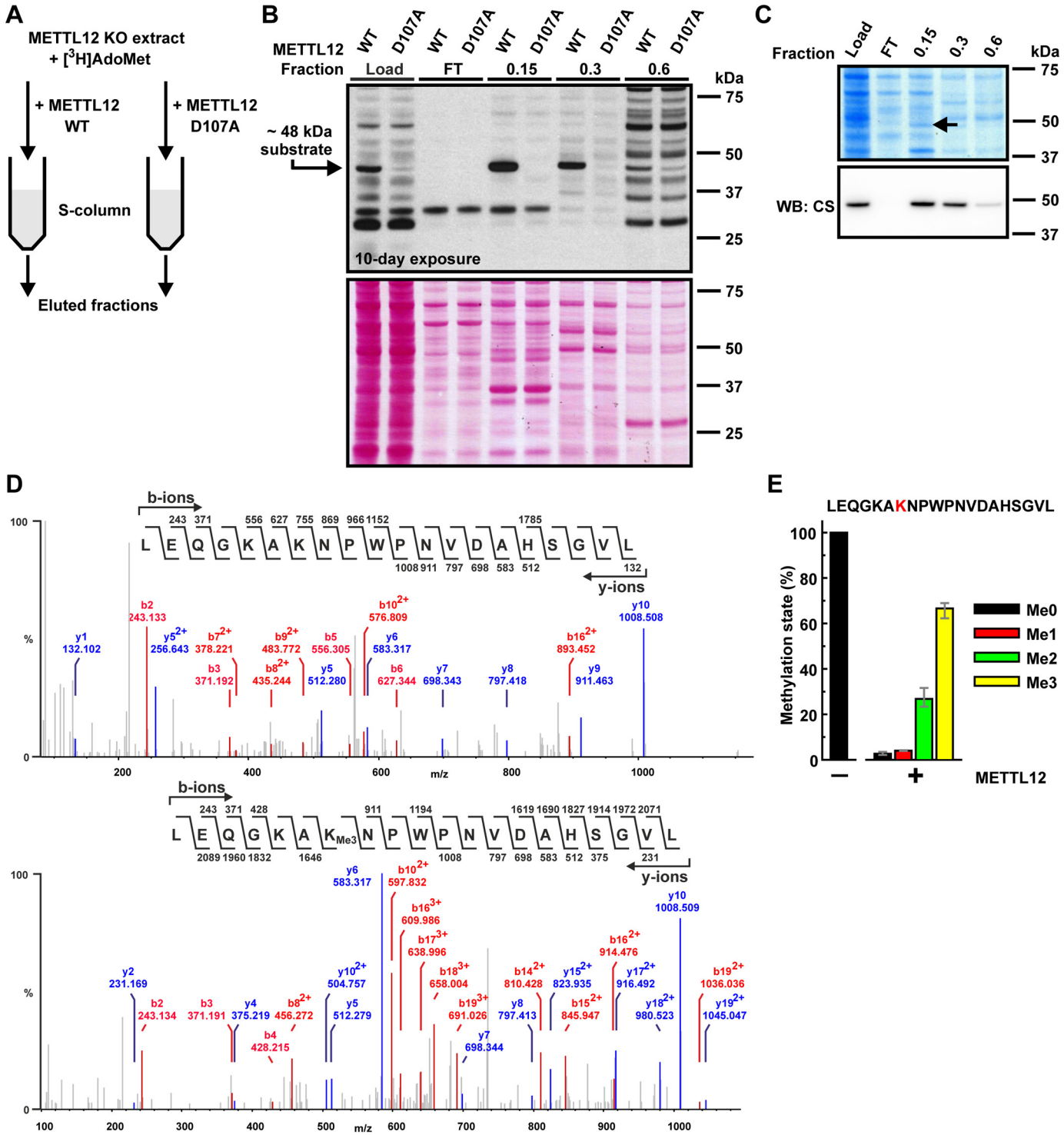

Figure 3. Identification of CS as candidate substrate for METTL12. *A*, schematics of chromatography-based strategy for enrichment of METTL12 substrate from cell extracts. Mitochondrial extracts from *METTL12* KO cells were incubated with [^{3}H]AdoMet and recombinant human METTL12, either WT or D107A mutant, and fractionated by cation-exchange (S-column) chromatography. *B*, enrichment of the ~48-kDa METTL12 substrate. Mitochondrial extracts were methylated and loaded onto an S-column according to the scheme depicted in *A*. Proteins were eluted from the S-column using a step-gradient of increasing NaCl ramped from 150 mM (0.15 fraction) to 600 mM (0.6 fraction). Eluted fractions were separated by SDS-PAGE, and [^{3}H]methyl incorporation into proteins was assessed by fluorography (*top*) of Ponceau S-stained membrane (*bottom*). *FT*, flow-through. *C*, SDS-PAGE analysis of cation-exchange fractions from *METTL12* KO cells. Mitochondrial extracts were fractionated by cation exchange, as in *B*, analyzed by SDS-PAGE, and stained with Coomassie (*top*) or analyzed by Western blot (*bottom*) and probed with anti-citrate synthase antibody (*WB: CS*). The *arrow* indicates the band corresponding to the ~48-kDa methylated substrate detected by fluorography, and MS analysis of this band revealed the presence of CS (Table 1). *D*, fragmentation mass spectra of chymotrypsin-generated peptide encompassing Leu-389–Leu-408 of CS, supporting the absence of Lys-395 methylation in *METTL12* KO cells (*top*) and the presence of trimethylated Lys-395 in METTL12-treated extracts from *METTL12* KO cells. *E*, CS is methylated at Lys-395 by recombinant METTL12. Mitochondrial extracts from *METTL12* KO cells were incubated with AdoMet without or with METTL12, fractionated by cation exchange, as in *B*, and CS present in 0.15 fraction was analyzed by MS. Shown are the relative intensities of MS signals gated for different methylation states of the indicated peptide (Lys-395 shown in *red*) from extracts untreated or treated with METTL12. *Error bars* indicate the range of values from three independent experiments.

Table 1
List of proteins identified in the ~48-kDa region of the 0.15 fraction of mitochondrial extract from *METTL12* KO cells
Mito, mitochondria; Cyto, cytosol; ER, endoplasmic reticulum; Nucl, nucleus.

Protein name	Accession number	Score	Coverage	Molecular mass[a]	Subcellular localization
			%	*kDa*	
Elongation factor Tu, mitochondrial	P49411	59.90	45.93	49.5	Mito
Citrate synthase, mitochondrial	O75390	49.48	45.61	51.7	Mito
Phosphoglycerate kinase 1	P00558	42.48	52.76	44.6	Cyto
α-Enolase	P06733	39.17	41.71	47.2	Cyto
Cytochrome *b*-c1 complex subunit 2, mitochondrial	P22695	36.47	32.45	48.4	Mito
Eukaryotic initiation factor 4A-I	P60842	25.06	27.09	46.2	Cyto
Protein disulfide-isomerase A6	Q15084	24.88	33.18	48.1	ER
Spliceosome RNA helicase DDX39B	Q13838	23.82	20.79	49.0	Nucl
Cytochrome b-c1 complex subunit 1, mitochondrial	P31930	22.47	31.25	52.6	Mito
ATP-dependent RNA helicase DDX39A	O00148	22.07	18.27	49.1	Nucl/Cyto

[a] Molecular mass of precursor protein.

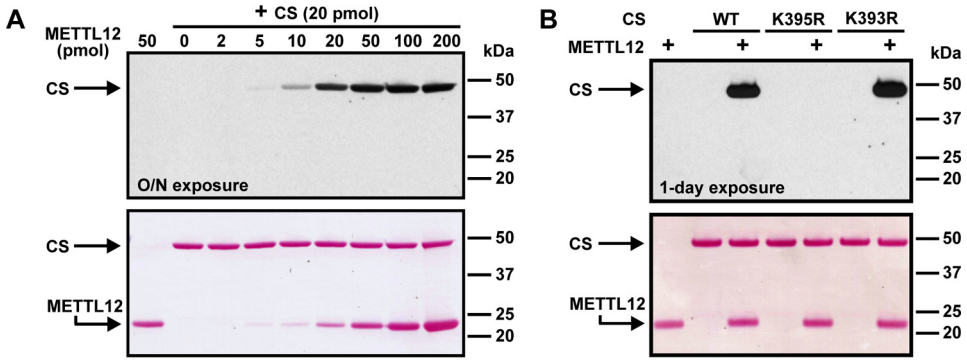

Figure 4. METTL12-mediated methylation of Lys-395 in recombinant CS *in vitro*. *A*, methylation of recombinant CS is dependent on METTL12. CS was incubated with [^{3}H]AdoMet and increasing amounts of METTL12, and [^{3}H]methyl incorporation was visualized by fluorography (*top*) of Ponceau S-stained membrane (*bottom*). *B*, evaluation of CS point mutants as substrates for METTL12-mediated methylation. CS, either wild-type (WT) or mutant (K395R or K393R), was incubated with [^{3}H]AdoMet and METTL12, and [^{3}H]-methyl incorporation was visualized by fluorography as in *A*.

ation was almost completely abolished by 100 μM AdoHcy. Importantly, the addition of AdoHcyase greatly alleviated the inhibitory effect of AdoHcy, and in agreement with the results in Fig. 5*B*, AdoHcyase increased methylation also in the absence of AdoHcy. The above results indicate that METTL12 has a much higher affinity for AdoHcy than for AdoMet and that AdoHcy, therefore, acts as a strong inhibitor of the enzyme, preventing enzymatic turnover.

We previously found for other 7BS KMTs that the efficiency of lysine methylation could be modulated by the specific binding of various ligands to the substrate (15, 18, 20). We, therefore, tested the effect of relevant metabolites, *i.e.* the CS substrates OAA and acetyl-CoA, as well as the product citrate on METTL12-mediated CS methylation. We found that OAA had a strong inhibitory effect on METTL12-dependent methylation of CS, *i.e.* methylation was inhibited by ~80% at 200 μM OAA (Fig. 6*A*), whereas neither acetyl-CoA nor citrate had any effect (Fig. 6*B*). Taken together, the data presented above indicate that METTL12 methylates CS in a non-processive reaction, which is inhibited by AdoHcy and OAA.

Modulation of CS activity by METTL12 in vitro

The crystal structure of pig CS shows that Lys-395 is localized close to the active site of the enzyme (30), suggesting that CS activity may be affected by METTL12-mediated methylation. To test this, we incubated CS with METTL12 in the presence of AdoMet and then measured the enzymatic activity of CS. Corresponding samples, where AdoMet had been omitted or replaced by AdoHcy, were included as negative controls. Interestingly, when CS was incubated with METTL12 in the presence of AdoMet, a substantial (~30%) reduction in CS activity was observed relative to the negative controls (Fig. 7*A*). Notably, no such effect was observed when the inactive METTL12 mutant (D107A) was used (we confirmed that this mutant enzyme was also inactive on recombinant CS; see supplemental Fig. S2). Taken together, these experiments indicate that METTL12-mediated methylation causes a small, but significant, reduction in CS activity.

To determine how METTL12-mediated methylation of CS affected the kinetics of the CS reaction, we measured the velocity of the CS-catalyzed reaction as a function of increasing OAA concentration while keeping the concentration of acetyl-CoA constant. These titration experiments were performed in parallel for methylated CS (incubated with AdoMet and METTL12 wild type) and unmethylated CS (incubated with AdoMet and METTL12 D107A mutant). Although the overall shape of the saturation curves was similar in the two cases, the apparent maximum velocity of the reaction was reduced for methylated CS compared with unmethylated CS (Fig. 7*B*). These results indicate that METTL12-mediated methylation primarily affects the rate constant of the CS-catalyzed reaction while having less effect on the affinity of CS for OAA.

METTL12 is responsible for CS methylation in vivo

We showed that recombinant METTL12 catalyzed methylation of CS at Lys-395 *in vitro*, both on recombinant CS and on

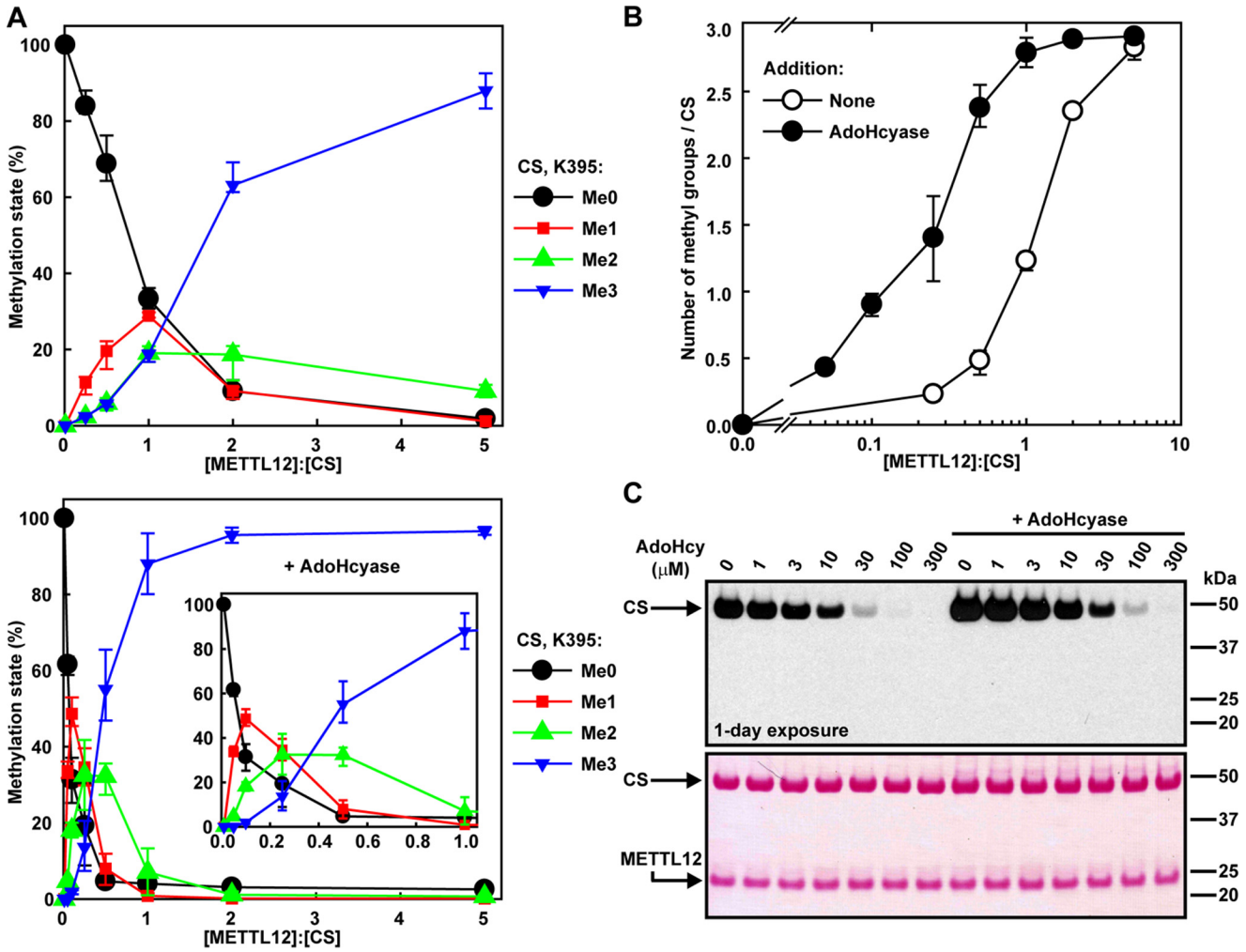

Figure 5. METTL12 is a non-processive enzyme strongly inhibited by AdoHcy. *A*, METTL12 is a non-processive enzyme. Recombinant CS was incubated with AdoMet and METTL12 at varying METTL12:CS ratios in the absence (*top*) or presence (*bottom*) of AdoHcyase. Methylation status of Lys-395 in CS was quantified by MS, similarly as in Fig. 3, *D* and *E*. Shown are the relative intensities of MS signals gated for different methylation states of peptides encompassing Lys-395, with *error bars* indicating the range of values from three (*top*) or two (*bottom*) independent experiments. The *inset* in the *lower panel* represents a blowup showing data for METTL12:CS values <1. *B*, results obtained in *A* expressed as the average number of methyl groups present on Lys-395 in CS. *C*, the effect of AdoHcy and AdoHcyase on METTL12-dependent methylation of CS. CS (2 μM) was incubated with METTL12 (2 μM), [^{3}H]AdoMet ([AdoMet]$_{total}$ = 32.6 μM), and varying amounts of AdoHcy in the absence or presence of AdoHcyase. [^{3}H]Methyl incorporation was visualized by fluorography (*top*) of Ponceau S-stained membrane (*bottom*).

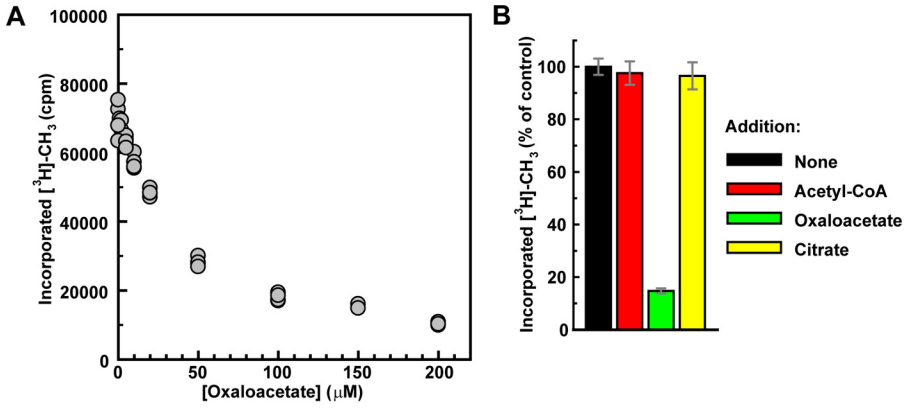

Figure 6. METTL12-dependent methylation of CS is inhibited by OAA. *A*, OAA inhibits METTL12-dependent methylation of CS. CS was incubated with METTL12, [^{3}H]AdoMet, and varying amounts of OAA. [^{3}H]Methyl incorporation into CS was assayed by scintillation counting of trichloroacetic acid-precipitated material. The experiment was repeated three times, with duplicate samples, and all data points are shown. *B*, methylation of CS is inhibited by OAA but not by citrate or acetyl-CoA. CS was incubated with METTL12 and [^{3}H]AdoMet in the absence or presence of acetyl-CoA, OAA, or citrate (200 μM each). [^{3}H]Methyl incorporation into CS was assayed as in *A*. Data are expressed as % of control (no addition). *Error bars* indicate the standard deviation (n = 8).

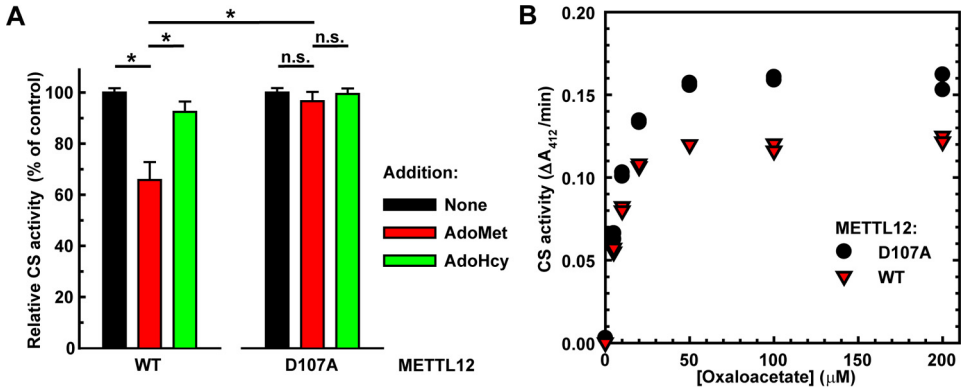

Figure 7. Impact of METTL12-dependent methylation on the activity of CS *in vitro*. *A*, CS activity is reduced by METTL12-mediated methylation. CS (0.5 μM) was incubated with METTL12 (2 μM), either wild-type (WT) or D107A mutant, and in the absence or presence of AdoMet or AdoHcy (1 mM each). Note: approximately 80% of CS became trimethylated under these conditions, as indicated in Fig. 5*A*. Reactions were diluted 250× with storage buffer containing DTNB (100 μM) and acetyl-CoA (300 μM), and CS activity was assayed by measuring the rate of TNB formation after adding OAA (300 μM). Values from three independent experiments performed in triplicate were normalized relative to CS activity observed in the presence of WT METTL12 in the absence of added co-factor (AdoMet or AdoHcy). *Bars* indicate standard deviation ($n = 9$). *, p value < 0.001; *n.s.*, not significant. *B*, METTL12-mediated methylation reduces CS maximum velocity. CS was incubated with AdoMet and METTL12, either wild-type or D107A mutant, conditions as in *A*, and CS activity was assayed similarly as in *A* by measuring TNB formation after the addition of varying amounts of OAA while keeping acetyl-CoA concentration constant (300 μM). CS activity is expressed as change in absorption at 412 nm/min (ΔA_{412}/min). Results from a representative experiment (of three) are shown.

CS from *METTL12* KO extracts. Taken together with the published observation that CS from pig heart is trimethylated on Lys-395, this indicates that METTL12 is responsible for CS methylation also *in vivo*. To firmly establish this, we assessed the methylation status of Lys-395 in CS in "wild-type" and *METTL12* KO HAP1 cells as well as in KO cells that had been complemented (supplemental Fig. S3) with ectopically expressed genes encoding either wild-type METTL12 or the enzymatically inactive mutant (D107A). We found that Lys-395 was predominantly trimethylated in the WT cells, with only small amounts of the un-, mono-, and dimethylated forms being detected (Fig. 8*A*). In contrast and as already shown, Lys-395 was exclusively observed in the unmethylated state in the *METTL12* KO cells (Fig. 8*A*). Reassuringly, complementation with an expression plasmid carrying the wild-type *METTL12* cDNA restored methylation in the KO cells, whereas no such effect was observed with the D107A-mutated cDNA. Taken together with the results from *in vitro* experiments, these data firmly establish that enzymatic activity of METTL12 is necessary and sufficient for CS methylation *in vivo*.

Methylation level of Lys-395 in CS differs between cell lines and various organs

Our *in vitro* experiments indicated that CS activity may be regulated by METTL12-mediated methylation in response to alterations in metabolite levels. To further address whether CS methylation is variable and, thus, likely to play a regulatory role, we analyzed CS Lys-395 methylation status in a panel of human cell lines as well as in several organs from pig. To this end we partially purified CS from the cells/organs using the purification scheme described previously (depicted in Fig. 3, *A* and *B*) and then assessed the methylation status of CS by MS. In the majority of cell lines tested, we observed high levels of Lys-395 methylation, with the trimethylated form (Me3) being predominant (>80%) (Fig. 8*B*). However, in HEK293 cells, CS showed a considerably lower methylation level, and a mixture of all four possible methylation states of Lys-395 was detected, *i.e.* unmethylated (Me0: ~36%), mono- (Me1: ~28%), di- (Me2: ~15%), and trimethylated (Me3: ~21%). In all analyzed pig organs (heart, muscle, liver, kidney, brain, ovary, uterus, small intestine, bone marrow, spleen) CS Lys-395 was exclusively found in the trimethylated form (data not shown).

Discussion

In the present study we have unraveled the biochemical function of the human MTase METTL12 using both *in vitro* and *in vivo* approaches. We found METTL12 to be localized to mitochondria and to methylate CS at Lys-395 in a non-processive fashion. Moreover, methylation reduced the activity of CS and was inhibited by the CS substrate OAA as well as by AdoHcy, suggesting that methylation may regulate CS function in response to altered metabolite levels.

We found that recombinant METTL12 methylated a single substrate of ~48 kDa in mitochondrial extracts. Partial purification of the extract followed by MS analysis identified several candidate substrates. These candidates included CS, which we subsequently established as a *bona fide* METTL12 substrate. Mitochondrial elongation factor Tu (TUFM) is another interesting candidate (Table 1) because it represents the mitochondrial ortholog of the cytosolic eEF1A, which is subject to methylation by the closest characterized mammalian homologues of METTL12, *i.e.* eEF1A-KMT2 and eEF1A-KMT4 (20, 21). Consequently, we have tested the activity of METTL12 on recombinant TUFM but were unable to detect any methylation, indicating that TUFM is not a substrate of METTL12.

While this manuscript was under preparation, a study from another group implicated METTL12 in methylation of CS (37). Using an antibody that recognized trimethylated lysine residues, various trimethyllysine-containing mitochondrial proteins were detected, and only one of these, subsequently identified as CS, lacked this modification in HAP1-derived *METTL12* KO cells. MS analysis demonstrated that Lys-395 in CS was unmethylated in the KO cells. Also, ectopic overexpression of METTL12 in HEK293 cells, where CS is relatively hypomethylated on Lys-395, resulted in a substantial increase in methylation. Although this study linked METTL12 to CS

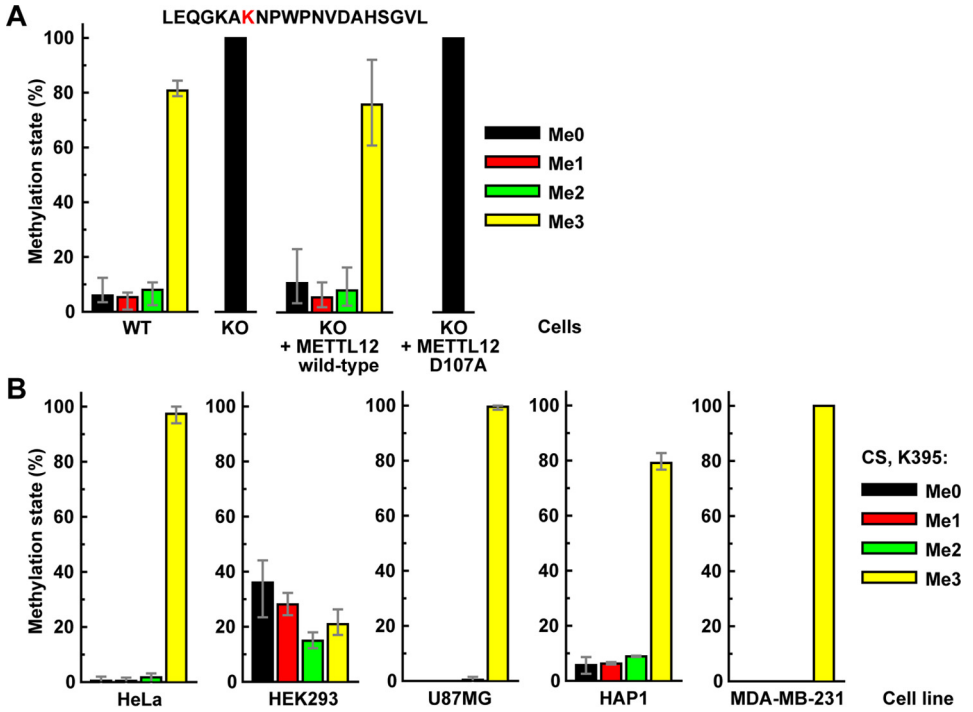

Figure 8. METTL12-mediated methylation of Lys-395 in CS *in vivo*. *A*, methylation of Lys-395 in CS is restored in *METTL12* KO cells complemented with *METTL12*. Shown is an MS analysis of Lys-395 methylation in CS from HAP1 WT or *METTL12* KO cells (*KO*) or KO cells expressing FLAG-tagged METTL12, either wild type or D107A mutant. Shown are the relative intensities of MS signals gated for different methylation states of the indicated peptide (Lys-395 shown in *red*). *Error bars* indicate the range of values from three independent analyses (WT and KO) or three independent clones of complemented cells, as indicated in supplemental Fig. S3. *B*, methylation status of Lys-395 in CS from various human cell lines. CS was enriched by cation-exchange (S-column) chromatography (as in Fig. 3, *A* and *B*), chymotrypsin-digested, and methylation of CS-derived peptides, encompassing Lys-395, was analyzed by MS. Shown are the relative intensities of MS signals gated for different methylation states of the peptides with *error bars* indicating the range of values from at least three independent experiments.

methylation *in vivo*, it was not demonstrated that METTL12 could catalyze CS methylation *in vitro*, and no functional effect of methylation was shown.

Cellular MTases differ greatly with respect to their affinities for the substrate AdoMet (expressed as the K_m value) and the potentially inhibitory product AdoHcy (expressed as the K_i value). Some MTases have an approximately equal affinity for AdoMet and AdoHcy (K_m (AdoMet) $\approx$ K_i (AdoHcy)) and others have a higher affinity for AdoMet (K_m (AdoMet) $<$ K_i (AdoHcy)), whereas others bind AdoHcy more avidly than AdoMet (K_m (AdoMet) $>$ K_i (AdoHcy)) (3). The latter category of MTases will be particularly prone to product inhibition by AdoHcy and sensitive to alterations in the [AdoMet]/[AdoHcy] ratio. Clarke and Banfield have compared K_m (AdoMet) and K_i (AdoHcy) values for 23 mammalian MTases (3), and the ones with the relatively highest affinity for AdoHcy displayed K_m (AdoMet)/K_i (AdoHcy) ratios in the range 25–30, which is comparable to METTL12 (the addition of only 1 μM AdoHcy inhibited METTL12 activity substantially in the presence of 32.6 μM of AdoMet; Fig. 5*C*). Thus, METTL12 appears, compared with most other mammalian MTases, to be highly sensitive toward alterations in the cellular [AdoMet]/[AdoHcy] ratio. This was also supported by the observation that METTL12 was unable to perform catalytic turnover unless AdoHcyase was added to the reaction mixture. Importantly, the AdoMet and AdoHcy concentrations used in our *in vitro* experiments are comparable with those found inside cells; typical cellular concentrations of AdoMet and AdoHcy lie within the ranges 10–100 μM and 0.1–20 μM, respectively (38). Interestingly, a number of recent studies have demonstrated that alterations in cellular metabolism leads to changes in the cellular AdoMet/AdoHcy ratio, which again causes changes in histone lysine methylation, thus providing an interesting link between metabolism and epigenetics (2, 40, 41). Similarly, our *in vitro* data suggest that CS activity may be modulated by AdoHcy-sensitive, METTL12-mediated lysine methylation in response to metabolic changes.

We found that the CS substrate OAA strongly inhibited METTL12-mediated methylation of CS, whereas no such effect was observed with either the co-substrate acetyl-CoA or with the product citrate. X-ray crystallographic studies have determined the structure of pig CS in complex with various metabolites, and CS exists in an "open" conformation in the absence of ligands or when complexed with citrate, whereas it adopts a "closed" conformation when complexed with OAA (30, 42). Only a minor portion of the CS structure is affected by the conformational switch between the closed and open states, but the methylation site Lys-395 is part of a segment that is shifted substantially (Fig. 9). This suggests that OAA exerts its inhibitory effect through inducing the closed conformation and, thereby, a repositioning of Lys-395 and surrounding residues.

We found that METTL12-mediated methylation caused a small, but significant, reduction in CS activity. In contrast, Rhein *et al.* (37) did not detect any difference in activity between CS isolated from wild-type and *METTL12* KO HAP1 cells, and another study did not detect significant differences in

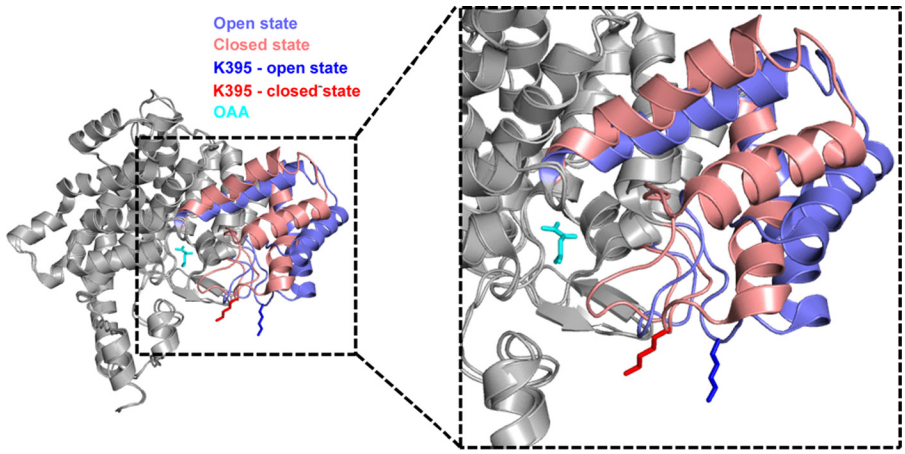

Figure 9. The methylation site Lys-395 shows a different position between open and closed states of CS. The regions of CS that show a similar structure between the open and closed states are shown in *gray*. For the regions that deviate between the two states, the open state is shown in *blue*, and the closed state in red. Stick representations are shown for OAA (*cyan*) and Lys-395 (*blue* in the open state, *red* in the closed state). The figure was generated by PyMOL Molecular Graphics System, Version 1.3 (Schrodinger, LLC) using available structures (PBD codes 1CTS and 4CTS) described previously (30, 42).

catalytic properties between recombinant pig CS, which is unmethylated, and CS from pig heart, which is trimethylated (43). However, in these two studies, the activity of CS from two different sources was compared (CS from WT *versus* KO cells; recombinant CS *versus* CS from pig heart), and this approach may be prone to uncertainties (*e.g.* variable loss of activity during enzyme isolation or inaccuracies in protein concentration determination) that could hinder the detection of small differences. In contrast, we used the same preparation of recombinant CS and then studied the effect of different additions (METTL12, AdoHcy, AdoMet), thus likely avoiding the above mentioned sources of error and allowing us to demonstrate a small, but robust, effect of methylation on CS activity; an effect that required the presence of both AdoMet and catalytically active METTL12. The small observed effect agrees well with the sketchy distribution of METTL12 in mammals, *e.g.* its absence in rats and mice, which also indicates that methylation is not strictly required for CS function but rather serves an optimizing or regulatory function that is beneficial under certain conditions.

We observed that CS was predominantly trimethylated in the tested human cell lines, except in HEK293 cells, where CS showed a much lower methylation level (Fig. 8*B*). Strikingly, we detected exclusively fully trimethylated CS in all analyzed pig organs, indicating that trimethylation of CS may represent the default state in METTL12-containing organisms. These observations further supports that methylation is important for CS function, but also raises the question of whether altered methylation actively regulates CS activity *in vivo*. It should be noted, however, that the analyzed organs came from a healthy, well fed pig, grown in a controlled environment. Thus, one may speculate that METTL12-mediated methylation may regulate CS activity under certain stress conditions (*e.g.* starvation or extensive exercise), thus playing a role in the adaptation to such conditions.

Bioinformatics analysis identified METTL12 as a member of a family of 7BS MTases, which also encompasses the human MTases eEF1A-KMT2 (gene name *EEF1AKMT2*; alias *METTL10*), eEF1A-KMT4 (gene name *EEF1AKMT4*; alias *ECE2*), and METTL13 (20). Including the present work, three of the four human members of this family have now been established as KMTs. This indicates that the remaining uncharacterized human member of this family, METTL13, is likely also a KMT. Numerous human 7BS MTases have been established as KMTs during the last years, and all of these are highly specific, *i.e.* only a single substrate has been identified, or in case of METTL21A, a group of highly related substrates (various Hsp70 proteins) (8, 13, 15, 39). Consequently, a naming nomenclature based on the substrate specificity has emerged for these enzymes. For example, the MTases enzymes METTL20 and FAM86A were found to target the β-subunit of the mitochondrial electron transfer flavoprotein (ETFβ) and eukaryotic elongation factor 2 (eEF2), respectively, and were consequently redubbed ETFβ-KMT and eEF2-KMT (gene names *EFTBKMT* and *EEF2KMT*) (14, 17). Thus, we suggest that METTL12 is renamed CS-KMT (gene name *CSKMT*) in keeping with this established nomenclature.

Author contributions—J. M., M. E. J., and P. Ø. F. conceived and planned the study. J. M., M. E. J., A. C. R., A. Y. Y. H. and P. Ø. F. planned the experiments. J. M., M. E. J., A. C. R., A. Y. Y. H., and A. M. performed the experiments. J. M. and P. Ø. F. wrote the manuscript. All authors analyzed data and read and commented on the manuscript.

Acknowledgments—We thank Eirin Helland (Norwegian Food Safety Authority) and Thomas Tollefsen (Fatland, Oslo) for assistance with acquiring samples from pig organs. We thank Oslo NorMIC Imaging Platform (Department of Biosciences, University of Oslo) for the use of cell imaging equipment.

References

1. Schubert, H. L., Blumenthal, R. M., and Cheng, X. (2003) Many paths to methyltransfer: a chronicle of convergence. *Trends Biochem. Sci.* **28,** 329–335
2. Mentch, S. J., and Locasale, J. W. (2016) One-carbon metabolism and epigenetics: understanding the specificity. *Ann. N.Y. Acad. Sci.* **1363,** 91–98

3. Clarke and Banfield, K. (2001) *S*-Adenosylmethionine-dependent methyltransferases. In *Homocysteine in Health and Disease* (Carmel, R., and Jacobsen, D. W., ed.), pp. 63–78, Cambridge University Press, Cambridge, UK
4. Bedford, M. T. (2007) Arginine methylation at a glance. *J. Cell Sci.* **120,** 4243–4246
5. Figaro, S., Scrima, N., Buckingham, R. H., and Heurgué-Hamard, V. (2008) HemK2 protein, encoded on human chromosome 21, methylates translation termination factor eRF1 *FEBS Lett.* **582,** 2352–2356
6. Lanouette, S., Mongeon, V., Figeys, D., and Couture, J. F. (2014) The functional diversity of protein lysine methylation. *Mol. Syst. Biol.* **10,** 724
7. Webb, K. J., Zurita-Lopez, C. I., Al-Hadid, Q., Laganowsky, A., Young, B. D., Lipson, R. S., Souda, P., Faull, K. F., Whitelegge, J. P., and Clarke, S. G. (2010) A novel 3-methylhistidine modification of yeast ribosomal protein Rpl3 is dependent upon the YIL110W methyltransferase. *J. Biol. Chem.* **285,** 37598–37606
8. Falnes, P. Ø., Jakobsson, M. E., Davydova, E., Ho, A., and Małecki, J. (2016) Protein lysine methylation by seven-β-strand methyltransferases. *Biochem. J.* **473,** 1995–2009
9. Herz, H. M., Garruss, A., and Shilatifard, A. (2013) SET for life: biochemical activities and biological functions of SET domain-containing proteins. *Trends Biochem. Sci.* **38,** 621–639
10. Moore, K. E., and Gozani, O. (2014) An unexpected journey: Lysine methylation across the proteome. *Biochim. Biophys. Acta* **1839,** 1395–1403
11. Greer, E. L., and Shi, Y. (2012) Histone methylation: a dynamic mark in health, disease and inheritance. *Nat. Rev. Genet.* **13,** 343–357
12. Kernstock, S., Davydova, E., Jakobsson, M., Moen, A., Pettersen, S., Mælandsmo, G. M., Egge-Jacobsen, W., and Falnes, P. Ø. (2012) Lysine methylation of VCP by a member of a novel human protein methyltransferase family. *Nat. Commun.* **3,** 1038
13. Cloutier, P., Lavallée-Adam, M., Faubert, D., Blanchette, M., and Coulombe, B. (2013) A newly uncovered group of distantly related lysine methyltransferases preferentially interact with molecular chaperones to regulate their activity. *PLoS Genet.* **9,** e1003210
14. Davydova, E., Ho, A. Y., Malecki, J., Moen, A., Enserink, J. M., Jakobsson, M. E., Loenarz, C., and Falnes, P. Ø. (2014) Identification and characterization of a novel evolutionarily conserved lysine-specific methyltransferase targeting eukaryotic translation elongation factor 2 (eEF2) *J. Biol. Chem.* **289,** 30499–30510
15. Jakobsson, M. E., Moen, A., Bousset, L., Egge-Jacobsen, W., Kernstock, S., Melki, R., and Falnes, P. Ø. (2013) Identification and characterization of a novel human methyltransferase modulating Hsp70 function through lysine methylation. *J. Biol. Chem.* **288,** 27752–27763
16. Magnani, R., Dirk, L. M., Trievel, R. C., and Houtz, R. L. (2010) Calmodulin methyltransferase is an evolutionarily conserved enzyme that trimethylates Lys-115 in calmodulin. *Nat. Commun.* **1,** 1–6
17. Małecki, J., Ho, A. Y., Moen, A., Dahl, H. A., and Falnes, P. Ø. (2015) Human METTL20 is a mitochondrial lysine methyltransferase that targets the β subunit of electron transfer flavoprotein (ETFβ) and modulates its activity. *J. Biol. Chem.* **290,** 423–434
18. Malecki, J., Aileni, V. K., Ho, A. Y. Y., Schwarz, J., Moen, A., Sørensen, V., Nilges, B. S., Jakobsson, M. E., Leidel, S. A., and Falnes, P. Ø. (2017) The novel lysine specific methyltransferase METTL21B affects mRNA translation through inducible and dynamic methylation of Lys-165 in human eukaryotic elongation factor 1α (eEF1A) *Nucleic Acids Res.* **45,** 4370–4389
19. Rhein, V. F., Carroll, J., He, J., Ding, S., Fearnley, I. M., and Walker, J. E. (2014) Human METTL20 methylates lysine residues adjacent to the recognition loop of the electron transfer flavoprotein in mitochondria. *J. Biol. Chem.* **289,** 24640–24651
20. Jakobsson, M. E., Malecki, J., Nilges, B. S., Moen, A., Leidel, S. A., and Falnes, P. Ø. (2017) Methylation of human eukaryotic elongation factor α (eEF1A) by a member of a novel protein lysine methyltransferase family modulates mRNA translation. *Nucleic Acids Res.* **45,** 8239–8254
21. Shimazu, T., Barjau, J., Sohtome, Y., Sodeoka, M., and Shinkai, Y. (2014) Selenium-based S-adenosylmethionine analog reveals the mammalian seven-β-strand methyltransferase METTL10 to be an EF1A1 lysine methyltransferase. *PLoS ONE* **9,** e105394
22. Hornbeck, P. V., Kornhauser, J. M., Tkachev, S., Zhang, B., Skrzypek, E., Murray, B., Latham, V., and Sullivan, M. (2012) PhosphoSitePlus: a comprehensive resource for investigating the structure and function of experimentally determined post-translational modifications in man and mouse. *Nucleic Acids Res.* **40,** D261–D270
23. Rhein, V. F., Carroll, J., Ding, S., Fearnley, I. M., and Walker, J. E. (2013) NDUFAF7 methylates arginine 85 in the NDUFS2 subunit of human complex I. *J. Biol. Chem.* **288,** 33016–33026
24. Wiegand, G., and Remington, S. J. (1986) Citrate synthase: structure, control, and mechanism. *Annu. Rev. Biophys. Biophys. Chem.* **15,** 97–117
25. Beeckmans, S. (1984) Some structural and regulatory aspects of citrate synthase. *Int. J. Biochem.* **16,** 341–351
26. Srere, P. A. (1974) Controls of citrate synthase activity. *Life Sci.* **15,** 1695–1710
27. LaNoue, K. F., Bryla, J., and Williamson, J. R. (1972) Feedback interactions in the control of citric acid cycle activity in rat heart mitochondria. *J. Biol. Chem.* **247,** 667–679
28. Smith, C. M., and Williamson, J. R. (1971) Inhibition of citrate synthase by succinyl-CoA and other metabolites. *FEBS Lett.* **18,** 35–38
29. Bloxham, D. P., Parmelee, D. C., Kumar, S., Walsh, K. A., and Titani, K. (1982) Complete amino acid sequence of porcine heart citrate synthase. *Biochemistry* **21,** 2028–2036
30. Remington, S., Wiegand, G., and Huber, R. (1982) Crystallographic refinement and atomic models of two different forms of citrate synthase at 2.7 and 1.7 A resolution. *J. Mol. Biol.* **158,** 111–152
31. McGinnis, S., and Madden, T. L. (2004) BLAST: at the core of a powerful and diverse set of sequence analysis tools. *Nucleic Acids Res.* **32,** W20–W25
32. Waterhouse, A. M., Procter, J. B., Martin, D. M., Clamp, M., and Barton, G. J. (2009) Jalview Version 2–a multiple sequence alignment editor and analysis workbench. *Bioinformatics.* **25,** 1189–1191
33. Małecki, J., Dahl, H. A., Moen, A., Davydova, E., and Falnes, P. Ø. (2016) The METTL20 homologue from *Agrobacterium tumefaciens* is a dual-specificity protein-lysine methyltransferase that targets ribosomal protein L7/L12 and the $\boldsymbol{\beta}$ subunit of electron transfer flavoprotein (ETF$\boldsymbol{\beta}$) *J. Biol. Chem.* **291,** 9581–9595
34. Srere, P. A. (1969) Citrate synthase. *Methods Enzymol.* **13,** 3–11
35. Petrossian, T. C., and Clarke, S. G. (2009) Multiple motif scanning to identify methyltransferases from the yeast proteome. *Mol. Cell. Proteomics* **8,** 1516–1526
36. Claros, M. G., and Vincens, P. (1996) Computational method to predict mitochondrially imported proteins and their targeting sequences. *Eur. J. Biochem.* **241,** 779–786
37. Rhein, V. F., Carroll, J., Ding, S., Fearnley, I. M., and Walker, J. E. (2017) Human METTL12 is a mitochondrial methyltransferase that modifies citrate synthase. *FEBS Lett.* **591,** 1641–1652
38. Fan, J., Krautkramer, K. A., Feldman, J. L., and Denu, J. M. (2015) Metabolic regulation of histone post-translational modifications. *ACS Chem. Biol.* **10,** 95–108
39. Jakobsson, M. E., Moen, A., and Falnes, P. Ø. (2016) Correspondence: On the enzymology and significance of HSPA1 lysine methylation. *Nat. Commun.* **7,** 11464
40. Shyh-Chang, N., Locasale, J. W., Lyssiotis, C. A., Zheng, Y., Teo, R. Y., Ratanasirintrawoot, S., Zhang, J., Onder, T., Unternaehrer, J. J., Zhu, H., Asara, J. M., Daley, G. Q., and Cantley, L. C. (2013) Influence of threonine metabolism on *S*-adenosylmethionine and histone methylation. *Science* **339,** 222–226
41. Ulanovskaya, O. A., Zuhl, A. M., and Cravatt, B. F. (2013) NNMT promotes epigenetic remodeling in cancer by creating a metabolic methylation sink. *Nat. Chem. Biol.* **9,** 300–306
42. Wiegand, G., Remington, S., Deisenhofer, J., and Huber, R. (1984) Crystal structure analysis and molecular model of a complex of citrate synthase with oxaloacetate and *S*-acetonyl-coenzyme A. *J. Mol. Biol.* **174,** 205–219
43. Evans, C. T., Owens, D. D., Slaughter, C. A., and Srere, P. A. (1988) Characterization of mutant TMK368K pig citrate synthase expressed in and isolated from *Escherichia coli*. *Biochem. Biophys. Res. Commun.* **157,** 1231–1238